REPRINTED FROM:

CHEMICAL PHYSICS

Chemical Physics 178 (1993) 377–385
North-Holland

Laser excitation and emission spectroscopy of the methoxy radical in a supersonic jet

Prabhakar Misra *, Xinming Zhu, Ching-Yu Hsueh
Laser Spectroscopy Laboratory, Department of Physics and Astronomy, Howard University, Washington, DC 20059, USA

and

Joshua B. Halpern
Laser Chemistry Laboratory, Department of Chemistry, Howard University, Washington, DC 20059, USA

Received 3 December 1992; in final form 16 July 1993

NORTH-HOLLAND
AMSTERDAM – LONDON – NEW YORK – TOKYO

Chemical Physics 178 (1993) 377–385
North-Holland

Laser excitation and emission spectroscopy of the methoxy radical in a supersonic jet

Prabhakar Misra *, Xinming Zhu, Ching-Yu Hsueh
Laser Spectroscopy Laboratory, Department of Physics and Astronomy, Howard University, Washington, DC 20059, USA

and

Joshua B. Halpern
Laser Chemistry Laboratory, Department of Chemistry, Howard University, Washington, DC 20059, USA

Received 3 December 1992; in final form 16 July 1993

Laser-induced excitation and wavelength-resolved emission spectra of the methoxy (CH_3O) radical have been obtained in a supersonic jet environment. Fluorescence in the near ultraviolet from several vibronic bands belonging to the $\tilde{A}\,^2A_1$–$\tilde{X}\,^2E$ electronic system of CH_3O has been dispersed by a 0.6 m monochromator with a resolution of 0.3 nm. A complete set of vibrational frequencies with all assignments for the $\tilde{X}\,^2E$ state of CH_3O has been obtained. To the best of our knowledge, the dispersed spectra of CH_3O for the 2_0^2 and $2_0^1 3_0^1$ bands are presented here for the first time. The vibrational constants determined by a least-squares fit for the ν_3 mode are $\omega_e'' = 1071\ cm^{-1}$ and $\omega_e'' x_e'' = 8.4\ cm^{-1}$. For the Jahn–Teller active ν_6 mode, the vibrational and anharmonic constants $\omega_e'' = 786\ cm^{-1}$ and $\omega_e'' x_e'' = 55\ cm^{-1}$, respectively, have been obtained for the first time.

1. Introduction

The methoxy (CH_3O) radical is an important chemical intermediate in combustion and atmospheric reactions [1,2]. It also has astronomical significance because of its presence in interstellar space [3]. The spectroscopy of CH_3O built around the $\tilde{A}\,^2A_1$–$\tilde{X}\,^2E$ electronic transition is intriguing on account of the orbitally degenerate ground state $\tilde{X}\,^2E$ [4], whereby the molecule exhibits Jahn–Teller distortion, Coriolis coupling and hyperfine structure [5,6]. A first order Jahn–Teller effect causes a spontaneous breaking of the nominal C_{3v} symmetry in CH_3O [7]. A quenched electronic angular momentum and the associated reduction in spin–orbit splitting [8] give rise to unusual spectral features for CH_3O. The spin–orbit interaction splits the ^2E level into two components $^2E_{1/2}$ and $^2E_{3/2}$. As a consequence, any vibronic level belonging to the upper $\tilde{A}\,^2A_1$ state can have transitions to both spin–orbit components of the $\tilde{X}\,^2E$ state. This is confirmed by the manifestation of spectral doublets in the vibronic spectrum of CH_3O [9].

Laser magnetic resonance investigations of Radford and Russell [10] in the far infrared and the microwave studies of Hirota et al. [11] have yielded considerable information about the ground ^2E state of CH_3O. Emission ascribed to the first excited state $^2A_1$ of CH_3O was first observed by Style and Ward [12] following the photolysis of CH_3ONO by a hydrogen continuum lamp and subsequently by Ohbayashi and coworkers [13] by the photodissociation of the same precursor using various vacuum-UV lamps. Wendt and Hunziker [14] recorded the electronic spectrum of CH_3O in absorption by using the modulated mercury-sensitized decomposition of $HCO{\cdot}OCH_3$. Several investigators [15–18] have used the technique of laser-induced fluorescence (LIF) to examine the $\tilde{A}\,^2A_1$–$\tilde{X}\,^2E$ electronic spectrum of CH_3O. LIF, in turn, has been combined with supersonic expansion [9,19–22] to study jet-cooled CH_3O radicals.

* Corresponding author.

Liu et al. [22] have performed a detailed rovibronic analysis of the 0_0^0 and 3_0^1 bands of CH_3O in the near ultraviolet. Foster et al. [9] have reported a comprehensive vibrational analysis relating to the LIF excitation and wavelength-resolved emission spectra of the $\tilde{A}\,^2A_1$–$\tilde{X}\,^2E$ system of CH_3O in a supersonic jet. Chiang et al. [23] reported four of six vibrational constants of CH_3O in solid argon. However, there still remains a certain measure of uncertainty [9] about some of the fundamental vibrational frequencies of CH_3O in both the $\tilde{A}$ and $\tilde{X}$ states. In this paper, we present a comprehensive vibronic analysis of the wavelength-resolved emission spectra corresponding to the $\tilde{A}\,^2A_1$–$\tilde{X}\,^2E$ system of CH_3O that extends the vibrational assignments of Foster et al. [9] and presents an analysis of the dispersed fluorescence spectra of the 2_0^2 and $2_0^1 3_0^1$ bands of the $\tilde{A}$–$\tilde{X}$ electronic system of CH_3O for the first time. In addition, there is an important departure from Foster et al.'s assignment of the vibrational intervals relative to an origin that is midway between the spin–orbit doublet (corresponding to half the separation between the $\tilde{X}\,^2E_{1/2}$ and $\tilde{X}\,^2E_{3/2}$ states) at the pump frequency of a vibronic band involving a symmetric mode. The observed vibrational intervals have been carefully separated into two groups, one corresponding to the $\tilde{A}\,^2A_1$–$\tilde{X}\,^2E_{3/2}$ transition and the other to $\tilde{A}\,^2A_1$–$\tilde{X}\,^2E_{1/2}$ so as to assign precisely the single lines corresponding to the Jahn–Teller active e vibrations. Moreover, such an approach for the vibrational intervals makes assignments involving a combination of modes less ambiguous. Fluorescence from the $\tilde{A}\,^2A_1$ state was dispersed employing a 0.6 m monochromator with 0.3 nm resolution over a wider spectral region than reported in the previously cited study [9]. A complete set of vibrational frequencies has been obtained for the $\tilde{X}\,^2E$ state and the uncertainty in the assignments for the most part is estimated to be less than 25 cm^{-1}.

2. Experimental

The precursor for the methoxy (CH_3O) radical was methyl nitrite (CH_3ONO). It was synthesized by adopting the protocol established by Blatt [9,24]. The boiling point of the methyl nitrite precursor is $-12°C$ [25]. A Fourier Transform infrared spectrum of the gaseous precursor showed infrared bands predominantly characteristic of methyl nitrite [26]. The sample was stored in liquid nitrogen until needed for the jet expansion.

Helium was used as a carrier gas and mixed with the methyl nitrite in the ratio 200:1 by volume. The mixture of helium and precursor (at a typical pressure of 10 to 14 atm) was introduced into a vacuum chamber through a commercial pulsed valve (General Valve IOTA ONE) of 0.5 mm orifice. The pressure in the evacuated chamber was typically $\sim 10^{-4}$ Torr and the open duration of the pulsed valve was set at 300 μs. Methyl nitrite seeded in the supersonic jet expansion was photolyzed by the KrF line at 248 nm of an excimer laser (Questek 2000). The excimer laser beam was focused into the expansion chamber by a quartz lens of focal length 750 mm, where the laser beam was set as close to the nozzle as possible. Methoxy molecules generated in situ in the supersonic expansion were then excited by a dye laser probe, which was a YAG (Quanta Ray DCR-11) pumped tunable dye laser [PDL-2] that was frequency-doubled to operate in the near UV. Both the YAG and excimer lasers were run at 10 Hz. Exciton dyes: KR620, Rh640 and DCM, were used to generate the requisite range of dye laser wavelengths. The linewidth afforded by the dye laser pulse was about 0.2 cm^{-1} and it could be reduced to 0.05 cm^{-1} by employing an etalon in the resonator cavity of the dye laser. Frequency-doubling was accomplished by a KDP crystal using an autotracker (Quanta Ray WEX-1A). The separation between the photolysis and probe lasers was typically 10–12 mm within the jet stream. Laser-induced fluorescence from the excited methoxy radicals was collected by a quartz lens at right angles to the plane containing the counterpropagating laser beams and the supersonic nozzle and was detected by a photomultiplier tube (EMI 9658R). Fluorescence excitation spectra for the methoxy radical were recorded by scanning the dye laser wavelength. The signals were accumulated and averaged by a boxcar integrator (Stanford Research Systems Model 250) with a gate-width of 0.5 μs in conjunction with an IBM/XT microcomputer-aided data acquisition system. Frequency calibration was accomplished by simultaneously recording the well-known $B\,^3\Pi_{0u}^+$–$X\,^1\Sigma_g^+$ electronic system [27] of I_2 in absorption with the dye laser fundamental while observing

the CH_3O spectrum with the doubled output. An iodine cell of 1.2 m length was used in the double-pass mode and kept at room temperature. Iodine lines were identified with the aid of an atlas [27] and the absolute wavenumbers for the rotational transitions of the $\tilde{A}$–$\tilde{X}$ system of methoxy were generated by a least-squares fit using the known iodine transitions.

To obtain the information concerning the vibrational intervals in the ground state, the dye laser was tuned to the wavelength where the radical emitted the strongest fluorescence in a certain chosen vibronic band. Single vibronic level dispersed fluorescence spectra were recorded by focusing the total fluorescence onto the entrance slit of a scanning 0.6 meter monochromator (Jobin Yvon HRS 2). Output signal at the exit slit was collected by a photomultiplier tube (Hamamatsu R905) and was relayed to a data acquisition system. The gate-width of the boxcar integrator used was typically 3 μs. The resolution of the monochromator was estimated to be 0.3 nm for a slit-width of 0.2 mm. Each data point was an average over 10 events and the scan speed for the grating was set at 24 Å per minute. The monochromator was calibrated by using mercury lines. With a mercury lamp in front of the entrance slit (0.025 mm wide), the monochromator was scanned from 290 to 400 nm. In this wavelength region, ten intense and well-known mercury transitions were recognized [28]. After a least-squares fit (using the commercial software EasyPlot), an equation relating the readings of the monochromator dial to the calibrated wavenumbers for the dispersed fluorescence spectra for CH_3O was obtained.

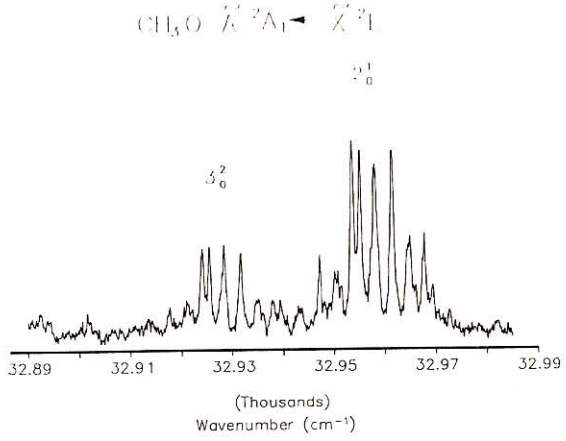

Fig. 1. Laser excitation spectrum of CH_3O showing the 3_0^2 and 2_0^1 bands. The helium backing pressure was 120 psi and the time delay between the photolysis and probe lasers was 10 μs.

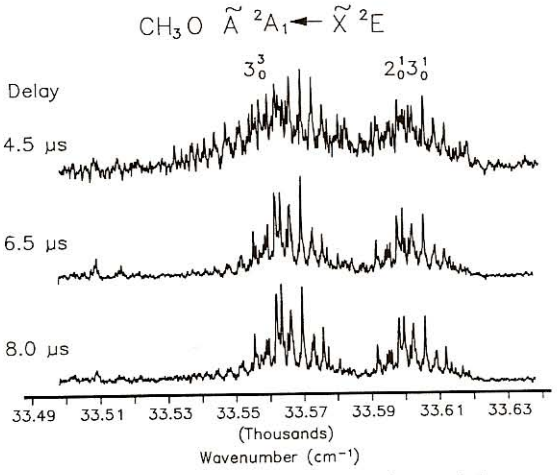

Fig. 2. Laser excitation scans showing the 3_0^3 and $2_0^1 3_0^1$ bands of CH_3O obtained with 120 psi helium backing pressure for three separate time delays of 4.5, 6.5 and 8.0 μs, respectively, between the photolysis and probe lasers.

3. Results and discussion

Fig. 1 is an illustration of the 32890–32990 cm^{-1} region of a typical LIF excitation spectrum of jet-cooled CH_3O obtained at a resolution of 0.2 cm^{-1}. The backing pressure of the helium and nitrite mixture behind the pulsed valve was 120 psi and the time delay between the photolysis and probe lasers was 10 μs. Fig. 1 shows the 3_0^2 band around 32930 cm^{-1} and the 2_0^1 band in the vicinity of 32960 cm^{-1}. Three scans for the 3_0^3 and $2_0^1 3_0^1$ bands obtained with 120 psi backing pressure for three separate time delays of 4.5, 6.5 and 8.0 μs, respectively, between the photolysis and probe lasers are shown in fig. 2. Even a cursory examination of the three spectra indicates the cooling effect realized in the supersonic jet expansion for longer time delays. Longer the time delay between the two lasers, the greater the number of collisions that the methoxy radicals suffer with the helium particles comprising the carrier gas and lower the translational, vibrational and rotational temperatures in the jet expansion. For polyatomic molecules, like CH_3O,

increased cooling results in perceptibly enhanced spectral resolution as is abundantly clear in the spectra displayed in fig. 2.

Dispersed fluorescence spectra for seven vibronic bands: 2_0^1, 2_0^2, 3_0^1, 3_0^2, 3_0^3, 3_0^5, and $2_0^1 3_0^1$, are reported in this paper. Of these wavelength-resolved emission spectra, the 2_0^2 and $2_0^1 3_0^1$ bands are presented here for the first time. In addition, our analysis provides new vibrational intervals for the emission from the 2_0^1, 3_0^1, 3_0^2, 3_0^3 and 3_0^5 bands that span a wider frequency range than reported previously [9]. Four illustrative dispersed fluorescence scans are shown in figs. 3–6. The first peak on the left of each scan corresponds to a mixture of the pump laser wavelength and the fluorescence from the methoxy transition from the vibrational level in the excited state to that in the ground state. The third peak in figs. 3–6 is a doublet with an average separation of 64 cm^{-1} (see table 1) relative to the first peak and is characteristic of the spin–orbit splitting in the ground state. Of the six normal vibrational modes possible for CH_3O [9], two symmetric a_1 vibrations (ν_2'', ν_3'') and two doubly degenerate e vibrations (ν_5'', ν_6'') can be identified unambiguously in the single vibronic level dispersed fluorescence spectra. Two other vibrational frequencies (ν_1'' and ν_4'') can also be determined but with less certainty because the corresponding vibronic bands have low intensity and do not exhibit long progressions. The intensity variations of the spectral lines are

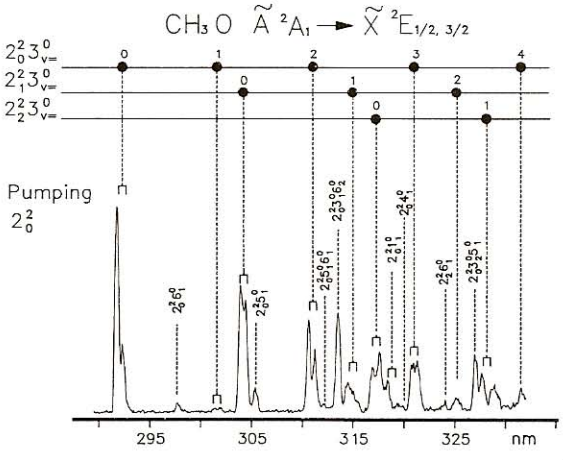

Fig. 3. Laser-excited dispersed fluorescence spectrum of the 2_0^2 band of CH_3O using a 0.6 m monochromator with 0.3 nm resolution.

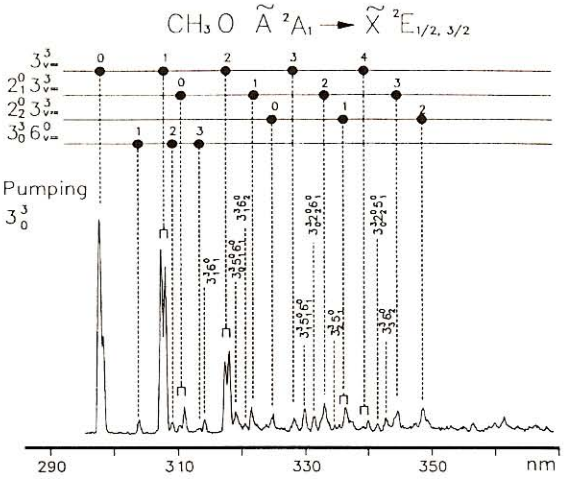

Fig. 4. Laser-excited dispersed fluorescence spectrum of the 3_0^3 band of CH_3O. Each data point was averaged over 10 events and the scan speed of the monochromator was set at 24 Å per minute.

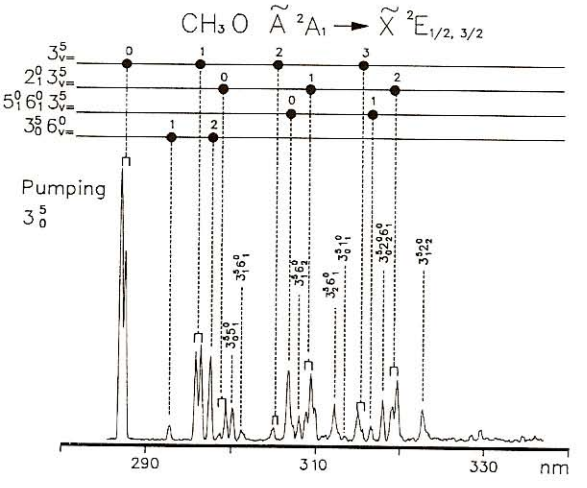

Fig. 5. Laser-excited dispersed fluorescence spectrum of CH_3O observed when the 3_0^5 band was pumped. Progressions in ν_3 and ν_6 were clearly visible.

due to changes in the Franck–Condon factors when different bands are pumped. A smooth envelope for the vibronic intensity pattern is clearly visible when progressions are followed to lower ν_3'' – as noted by earlier authors [9,14]; for example, the $2_0^1 3_{v''}^0$ progression shown in fig. 3 and the $3_{v''}^3$ progression in fig. 4 illustrate clearly these smooth contours. And yet the vibrational intervals remain essentially firm. An av-

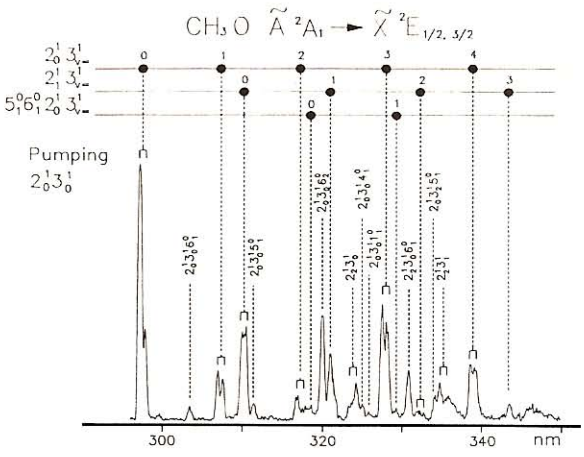

Fig. 6. Laser-excited dispersed fluorescence spectrum of CH_3O observed when the $2_0^1 3_0^1$ combination band was excited.

erage was taken over seven scans, and then a vibrational assignment was made corresponding to the mean wavenumber interval. The ν_3'' mode corresponding to the C-O symmetric stretch gives the strongest emission, and its "doubled progressions" are obvious; although the intensities of the members corresponding to the spin–orbit doublets vary. By "doubled progressions" is meant the consistent doubling of vibronic features in the dispersed spectrum – the doubling simply refers to the spin–orbit splitting of the ground state. The ν_2 emission is strong when the ν_2 mode (corresponding to the umbrella vibration) is pumped. Also, the ν_5 (scissor vibrational mode) and ν_6 (rocking mode) emissions are relatively stronger compared to those involving ν_1 (a_1 C–H stretch) and ν_4 (e C–H stretch). One can find the ν_5'' peaks when 2_0^1, 2_0^2, 3_0^1, 3_0^5, and $2_0^1 3_0^1$ bands are dispersed; while ν_6'' features are visible in 2_0^1, 2_0^2, 3_0^2, 3_0^3, 3_0^5, and $2_0^1 3_0^1$ wavelength-resolved emission spectra. Overtones of ν_6'' (for e.g. $2\nu_6''$ and $3\nu_6''$) are prominent in some of the recorded spectra (figs. 3–5). For instance, when the 3_0^5 band is pumped and dispersed, the $2\nu_6''$ peak appears as a strong spectral feature comparable in intensity to the ν_3'' peaks, and the $3\nu_6''$ line is also identifiable. The ν_1 and ν_4 vibrations show up as weak peaks. The vibrational assignments have been made using the fundamental ground state vibrational frequencies cited for CH_3O in the literature and those for similar symmetric top molecules. Frequencies assigned to the ν_1 and ν_4 modes were similar to those for CH_3F and CH_3Cl [29]. Since $\nu_4'' > \nu_1''$ for both CH_3F and CH_3Cl [29], our assigned fundamentals $\nu_4'' = 3020\ cm^{-1}$ and $\nu_1'' = 2869\ cm^{-1}$ for CH_3O are corroborated because they maintain such a relationship also. All transitions observed are listed in table 1, and their assignments are listed in table 2. The transitions from the upper $\tilde{A}\,^2A_1$ state to the lower $\tilde{X}\,^2E_{3/2}$ state have been collected and placed on the left in table 2, and those to the $\tilde{X}\,^2E_{1/2}$ state on the right. We did not take the origin of transitions to be the mean of the $\tilde{A}\,^2A_1$–$\tilde{X}\,^2E_{3/2}$ and $\tilde{A}\,^2A_1$–$\tilde{X}\,^2E_{1/2}$ excitation frequencies as employed in ref. [9], but separated them into two groups as indicated above, especially because the three e modes show up as single lines. The advantage of this approach becomes more obvious when it is used for the vibrational assignments relating to the CH_3S radical, where the magnitude of the spin–orbit splitting of the symmetric modes is as large as 257 cm^{-1} [30]. We have also made vibrational assignments using the above cited approach for CH_3S, which is being published elsewhere. All of the vibrational assignments are consistent to within a deviation that is less than 25 cm^{-1}, except for the 2535 cm^{-1} vibration that has a large deviation (exceeding 25 cm^{-1}) and is tagged with a question mark (?). This large deviation in vibrational interval is in all probability due to interaction between the umbrella (ν_2) and C–O symmetric stretch (ν_3) modes.

The total energy for a single vibrational mode, neglecting the rotational energy term, is given by [31]

$$T = T_e + \omega_e(v+\tfrac{1}{2}) - \omega_e x_e(v+\tfrac{1}{2})^2 + \dots , \qquad (1)$$

where T_e, ω_e, $\omega_e x_e$ and v are the electronic energy term, the vibrational constant, the anharmonic constant and the vibrational quantum number, respectively. The wave numbers of the spectral lines corresponding to the transitions between two electronic states are given by

$$\begin{aligned}\nu &= T' - T'' \\ &= T_e' - T_e'' + \omega_e'(v'+\tfrac{1}{2}) - \omega_e''(v''+\tfrac{1}{2}) \\ &\quad - \omega_e' x_e'(v'+\tfrac{1}{2})^2 + \omega_e'' x_e''(v''+\tfrac{1}{2})^2 + \dots , \qquad (2)\end{aligned}$$

where a single prime indicates the upper state, and a double prime denotes the lower state. When $v''=0$, $\nu = \nu_0$ yields the band origin ν_0. Thus, we have

Table 1
CH_3O $\tilde{X}$ ^2E vibrational intervals observed in dispersed fluorescence. The numbers listed are the differences between the pump frequency and the corresponding emission frequencies (in cm^{-1})

2_0^1	2_0^2	3_0^1	3_0^2	3_0^3	3_0^5	$2_0^1 3_0^1$	Average (cm^{-1})
65	63	55	80	68	57	75	64
695	690		674	693	689	687	688
1059	1099	1055	1072	1050	1035	1066	1062
1120	1165	1126	1127	1128	1104	1123	1128
			1248	1240	1232		1240
1381	1375	1382	1361	1372	1367	1388	1375
1434	1432	1446	1438	1441	1441	1437	1438
1527	1533	1522			1523	1534	1528
				1694			1694
1756		1760	1762	1762	1765		1760
2077	2088	2085	2103	2083	2061	2094	2084
2141	2149	2152	2153	2150		2151	2149
	2238			2248	2246	2255	2247
2386	2382	2379	2392	2392	2380	2390	2386
2485	2483	2486		2489	2471	2487	2484
	2538	2540			2527		2535
		2592			2569		2567
2726	2724					2708	2719
2798	2790					2801	2796
		2814	2822	2815	2823		2818
	2869					2873	2869
	2961				2945	2953	2953
	3020				3020		3020
3110	3110	3112	3116	3121	3107	3115	3113
3169	3156	3147	3163		3161	3164	3160
3264				3281	3260	3271	3269
3404	3424	3410	3416	3422	3399	3416	3413
3508	3519	3515	3532		3511	3526	3518
3560		3548		3561	3570		3560
3715	3695			3705		3712	3707
3772	3763	3766		3776		3772	3770
3863	3881	3831	3846	3859	3854	3872	3858
4109	4119		4109	4112		4113	4112
4159			4176	4180		4176	4173
				4306			4306
4400			4417	4420			4412
4530				4552		4525	4536
4740							4740
			4818	4812			4815
4902			4908	4906			4905
5101			5100				5101
5142							5142
			5428				5428
5514			5554	5540			5536
			5703				5703
			5812	5805			5808
			5944	5918			5931
6089							6089
6118							6118
6497							6497

Table 2
Vibrational assignments of the intervals observed in dispersed fluorescence of CH_3O $\tilde{X}\,^2E$. The numbers listed are differences between the pump frequency and the corresponding emission frequencies (in cm^{-1})

$\tilde{A}\,^2A_1$–$\tilde{X}\,^2E_{3/2}$	$\tilde{A}\,^2A_1$–$\tilde{X}\,^2E_{1/2}$	Assignment
0	64	
688		ν_6
1062	1128	ν_3
1240		$2\nu_6$
1375	1438	ν_2
1528		ν_5
1694		$3\nu_6$
1760		$\nu_3+\nu_6$
2084	2149	$2\nu_3$
2247		$\nu_5+\nu_6$
	2386	$\nu_3+2\nu_6$
	2484	$\nu_2+\nu_3$
2535		(?)
2567		$\nu_3+\nu_5$
2719	2796	$2\nu_2$
	2818	$2\nu_3+\nu_6$
2869	2953	ν_1
3020		ν_4
3113	3160	$3\nu_3$
	3269	$\nu_3+\nu_5+\nu_6$
3413		$2\nu_2+\nu_6$
	3518	$2\nu_3+\nu_2$
3560		$\nu_1+\nu_6$
3707		$\nu_4+\nu_6$
3770	3858	$\nu_3+2\nu_2$
4112	4173	$4\nu_3$
	4203	$\nu_2+2\nu_3+\nu_6$
	4306	$2\nu_2+\nu_5$
	4412	$3\nu_3+2\nu_6$
	4536	$3\nu_3+\nu_2$
	4740	$\nu_2+2\nu_3+2\nu_6$
4815	4905	$2\nu_3+2\nu_2$
5101	5142	$5\nu_3$
	5428	$4\nu_3+2\nu_6$
	5536	$4\nu_3+\nu_2$
	5703	$4\nu_3+\nu_5$
	5808	$5\nu_3+\nu_6$
	5931	$3\nu_3+2\nu_2$
6089	6118	$6\nu_3$
	6497	$5\nu_3+\nu_2$

$$\nu_0-\nu=(-\tfrac{1}{2}\omega''_e+\tfrac{1}{4}\omega''_e x''_e)+\omega''_e(v''+\tfrac{1}{2})-\omega''_e x''_e(v''+\tfrac{1}{2})^2 . \quad (3)$$

The observed average wavenumbers, which are also listed in table 1, were fitted by the least-squares technique to the above equation for $\nu_0-\nu$. The lines belonging to the ν_3 progression yield the vibrational constants $\omega''_3=1071\ cm^{-1}$ and $\omega''_3x''_3=8.4\ cm^{-1}$, and those part of the ν_6 progression gave $\omega''_6=786\ cm^{-1}$ and $\omega''_6x''_6=55\ cm^{-1}$. We were unable to fit similarly the other four vibrational modes because there were not adequate members forming progressions involving these vibrations. Some vibrational constants for the ν_3 mode determined in earlier studies [15,17,18,21] are listed in table 3 for comparison. The constants for the ν_6 mode are also listed in table 3 and to the best of our knowledge have been determined for the first time. Interestingly, the anharmonic constant $\omega''_6x''_6$ for the Jahn–Teller active ν_6 mode is about 6.5 times larger than $\omega''_3x''_3$. Table 4 summarizes the complete set of fundamental vibrational frequencies determined in the present study for the $\tilde{X}\,^2E$ state of CH_3O, which is compared with those for two other $\tilde{X}$ CH_3X (X=F, Cl) molecules and also with those for $\tilde{X}$ CH_3O cited in a previous work [9]. For the symmetric a_1 vibrations, the observed doublet progressions yield average vibrational intervals that help determine fundamental vibrational frequencies ν''_1, ν''_2 and ν''_3. The frequencies for ν''_2 and ν''_3 are consistent with earlier studies [9,23] and are within our experimental uncertainty of 25 cm^{-1}. However, ν''_1 has been a assigned a value 2869 cm^{-1} based on our data, and it compares reasonably well with $\nu''_1=2840\ cm^{-1}$ for $\tilde{X}$ CH_3O quoted in ref. [9]. For the asymmetric e vibrations, our analysis of the singlet progressions yield values for the fundamental vibrational frequencies ν''_4, ν''_5 and ν''_6. It needs to be emphasized that we have carefully separated (in table 2) the e progressions involving $\tilde{X}\,^2E_{3/2}$ and $\tilde{X}\,^2E_{1/2}$, respectively. In this manner, the present values for ν''_4, ν''_5 and ν''_6 can be compared directly with

Table 3
Vibrational constants (in cm^{-1}) for the ν_3 and ν_6 modes of the $\tilde{X}\,^2E$ state of CH_3O

ω''_3	$\omega''_3x''_3$	ω''_6	$\omega''_6x''_6$	Ref.
1022	3.2			[15]
1035	6.02			[17]
1064	9.5			[21]
1051	6.5			[18]
1071	8.4	786	55	this work

Table 4
Fundamental vibrational frequencies (in cm^{-1}) for $\tilde{X}$ CH_3O compared with those of $\tilde{X}$ CH_3F and $\tilde{X}$ CH_3Cl

Molecule	Mode						
	ν_1	ν_2	ν_3	ν_4	ν_5	ν_6	ref.
$\tilde{X}$ CH_3F	2965	1475	1048	2982	1471	1196	[29]
$\tilde{X}$ CH_3Cl	2966	1355	732	3042	1455	1015	[29]
$\tilde{X}$ CH_3O	2840	1362	1047	2774	1487	653	[9]
$\tilde{X}$ CH_3O	2869	1375	1062	3020	1528	688	this work

the average vibrational intervals derived in ref. [9] (table 4) relative to the pump. Our values $\nu_5'' = 1528$ cm^{-1} and $\nu_6'' = 688$ cm^{-1} compare well with the values $\nu_5'' = 1519$ cm^{-1} and $\nu_6'' = 685$ cm^{-1} relative to the pump given in ref. [9]. However, ν_4'' was not determined well in ref. [9] (it was mentioned to be 2774? in table 4). On the basis of our new data, we reassign a new value 3020 cm^{-1} to ν_4'' for $\tilde{X}$ CH_3O, which compares well with $\nu_4'' = 3044$ cm^{-1} for $\tilde{X}$ CH_3Cl. Our present study also determines for the first time several overtone vibrational frequencies (for e.g., $4\nu_3''$, $5\nu_3''$ and $6\nu_3''$) as indicated in table 2) for the $\tilde{X}$ ^2E state of methoxy.

Acknowledgement

The research work reported here was supported by Wright-Patterson Air Force Base (Grant No. F33615-90-C-2038), the Collaborative Core Unit of Howard University's Graduate School of Arts and Sciences, and the National Aeronautics and Space Administration Center for Terrestrial and Extraterrestrial Atmospheres (Grant No. NASA NAGW-2950).

References

[1] K.L. Demerjian, J.A. Kerr and J.G. Calvert, Advan. Environ. Sci. Technol. 4 (1974) 1.
[2] P.H. Leighton, Photochemistry of air pollution (Academic Press, New York, 1961).
[3] A.C. Baldwin and D.M. Golden, Chem. Phys. Letters 55 (1978) 350.
[4] J.M. Brown, Mol. Phys. 20 (1971) 817.
[5] J.T. Hougen, J. Mol. Spectry. 81 (1980) 73.
[6] D.R. Yarkony, H.F. Schaefer III and S. Rothenberg, J. Am. Chem. Soc. 96 (1974) 656.
[7] H.A. Jahn and E. Teller, Proc. Roy. Soc. A 161 (1937) 220.
[8] P.G. Carrick, S.D. Brossard and P.C. Engelking, J. Chem. Phys. 83 (1985) 1995.
[9] S.C. Foster, P. Misra, T.-Y.D. Lin, C.P. Damo, C.C. Carter and T.A. Miller, J. Phys. Chem. 92 (1988) 5914.
[10] H.E. Radford and D.K. Russell, J. Chem. Phys. 66 (1977) 2222;
D.K. Russell and H.E. Radford, J. Chem. Phys. 72 (1980) 2750.
[11] Y. Endo, S. Saito and E. Hirota, J. Chem. Phys. 81 (1984) 122;
T. Momose, Y. Endo, E. Hirota and T. Shida, J. Chem. Phys. 88 (1988) 5338.
[12] D.W.G. Style and J.C. Ward, Trans. Faraday Soc. 49 (1953) 999.
[13] K. Ohbayashi, H. Akimoto and I. Tanaka, J. Phys. Chem. 81 (1977) 798.
[14] H.R. Wendt and H.E. Hunziker, J. Chem. Phys. 71 (1979) 5202;
N.L. Garland and D.R. Crosley, J. Phys. Chem. 92 (1988) 5322.
[15] G. Inoue, H. Akimoto and M. Okuda, J. Chem. Phys. 72 (1980) 1769.
[16] N. Sanders, J.E. Butler, L.R. Pasternack and J.R. McDonald, Chem. Phys. 48 (1980) 203.
[17] T. Ebata, H. Yanagishita, K. Obi and I. Tanaka, Chem. Phys. 69 (1982) 27.
[18] S.-Y. Chiang, Y.-C. Hsu and Y.-P. Lee, J. Chem. Phys. 90 (1989) 81.
[19] D.E. Powers, J.B. Hopkins and R.E. Smalley, J. Phys. Chem. 85 (1981) 2711.
[20] K. Fuke, K. Ozawa and K. Kaya, Chem. Phys. Letters 126 (1986) 119.
[21] S.D. Brossard, P.G. Carrick, E.L. Chappell, S.C. Hulegaard and P.C. Engelking, J. Chem. Phys. 84 (1986) 2459.
[22] X. Liu, C.P. Damo, T.-Y.D. Lin, S.C. Foster, P. Misra, L. Yu and T.A. Miller, J. Phys. Chem. 93 (1989) 2266.
[23] S.-Y. Chiang, Y.-C. Hsu and Y.-P. Lee, J. Chem. Phys. 90 (1989) 81.
[24] A.H. Blatt, ed., Organic syntheses (Wiley, New York, 1943) Collective Vol. 2, p. 363.
[25] H.W. Thompson and F.S. Dainton, Trans. Faraday Soc. 33 (1937) 1546.
[26] F.L. Rook and M.E. Jacox, J. Mol. Spectry. 93 (1982) 101.

[27] S. Gerstenkorn and P. Luc, Atlas du spectre d'absorption de la molecule d'iode (CNRS, Paris, 1978) Part II.
[28] F.M. Phelps III, M.I.T. wavelength tables, Vol. 2. Wavelengths by element (MIT Press, Cambridge, MA, 1982).
[29] G. Herzberg, Molecular spectra and molecular structure, II. Infrared and Raman spectra of polyatomic molecules (Van Nostrand Reinhold, New York, 1945) p. 315.
[30] S.-Y. Chiang and Y.-P. Lee, J. Chem. Phys. 95 (1991) 66.
[31] G. Herzberg, Molecular spectra and molecular structure, III. Electronic spectra and electronic structure of polyatomic molecules. (Van Nostrand Reinhold, New York, 1966).